Spin Transition Complexes

International Edition: DOI: 10.1002/anie.201507620
German Edition: DOI: 10.1002/ange.201507620

# Meltable Spin Transition Molecular Materials with Tunable $T_c$ and Hysteresis Loop Width

*Tania Romero-Morcillo, Maksym Seredyuk,* M. Carmen Muñoz, and Jose A. Real**

***Abstract:*** *Herein, we report a way to achieve abrupt high-spin to low-spin transition with controllable transition temperature and hysteresis width, relying not on solid-state cooperative interactions, but utilizing coherency between phase and spin transitions in neutral $Fe^{II}$ meltable complexes.*

Much interest in the area of spin transition (ST) is focused on the bistability of systems exhibiting hysteresis, or memory effect, corresponding to two different spin states. Switching between the states, high spin (HS) and low spin (LS), occurs in a reversible and detectable way with concomitant variation of relevant physical magnitudes, including magnetic susceptibility, optical density,[1] dielectric constant,[2] and electric conductivity,[3] which constitute the background for possible exploitation of the ST compounds in technical devices. Intensive studies of the ST phenomenon made it clear that hysteretic behavior is dependent on interactions of individual metal centers with each other, both on intramolecular and intermolecular levels.[4] Efforts have thus been directed to enhance cooperativity in order to achieve abrupt transitions and significant bistability (supramolecular and polymeric approaches).[5] Despite understanding the role of cooperative interactions in defining the character of ST in solids,[6] the control of the transition temperature and, in the case of hysteretic transitions, the control of the hysteresis width are still the two greatest challenges remaining in the field. So far, the control of the transition temperature by chemical design was clearly demonstrated only for complexes $[Fe(trzH)_x(trzNH_2)_{3-x}](ClO_4)_2{\cdot}H_2O$ $(x = 0–3)$[7] and $[Fe(pyrazine)[Pt(CN)_4I_y]$ $(y = 0–1)$[8] by varying their composition. Other examples include inseparable variation of transition temperature and hysteresis width by isomorphic substitution,[9] application of external pressure,[10] or size reduction at nanoscale.[11]

The potential to control the spin state by a phase transition was demonstrated recently.[12] A bimodal reversible change from the LS state to the HS state at the $Fe^{II}$ sites is observed concomitantly with a reversible transition from crystalline to liquid crystalline state. This change of aggregation state upon melting is the driving force of a fairly incomplete ST (up to ca. 10% of $Fe^{II}$ ions).[12a,13] Having analyzed data reported up to now,[14] it has been assumed that the complex molecule has to suit several essential criteria to achieve more effective synchronicity between the phenomena. It should be: i) mononuclear complexes with aromatic planar substituents suitable for π-π interactions; ii) neutral to form a compact crystal lattice with strong intermolecular interactions; and iii) with optimal number of aliphatic substituents imparting controllable melting character to the compound.

Here, we report on the verification of this hypothesis. To do so, we have selected a suitable $Fe^{II}$ complex with functionalized asymmetric tridentate ligands *N′*-(1-(pyridin-2-yl)ethylidene)benzohydrazide, as previously reported.[15] Variations of the molecular structure allow coarse and fine-tuning of the reversible LS-HS spin transition with a remarkable hysteresis reflecting the structural phase transition behavior. Solubility in common organic solvent and easy processability of these soft matter compounds opens a way for their direct technical implementation.

The compounds under discussion have been synthesized by condensation of a functionalized hydrazone (**a**) with ketone (**b**) and subsequent reaction with $Fe^{II}$ ion in the presence of a base to afford alkyl-bearing complexes (**c**) (Scheme 1). To describe the obtained complexes, the nomen-

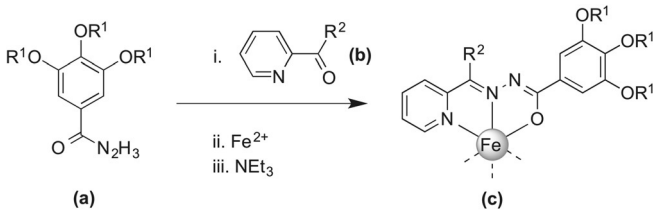


| R1 \ R2 | $CH_3$ | $C_2H_5$ | $C_3H_7$ | $C_4H_9$ | $C_5H_{11}$ |
|---|---|---|---|---|---|
| $CH_3$ | | | **1-3** | | |
| $C_4H_9$ | **4-1** | | | | |
| $C_8H_{17}$ | **8-1** | | | | |
| $C_{12}H_{25}$ | **12-1** | | | | |
| $C_{14}H_{29}$ | **14-1** | **14-2** | | **14-4** | **14-5** |
| $C_{16}H_{33}$ | **16-1** | | | | |

***Scheme 1.*** Synthesis of functionalized complexes.

[*] T. Romero-Morcillo, Dr. M. Seredyuk, Prof. Dr. J. A. Real
Instituto de Ciencia Molecular (ICMol), Universidad de Valencia
46980 Paterna, Valencia (Spain)
E-mail: jose.a.real@uv.es
Dr. M. Seredyuk
National Taras Shevchenko University
Department of Physical Chemistry
Volodymyrska Str. 64, Kiev 01601 (Ukraine)
E-mail: mcs@univ.kiev.ua
mlseredyuk@gmail.com
Prof. Dr. M. C. Muñoz
Departamento de Física Aplicada, Universitat Politècnica de València
46022, Valencia (Spain)

Supporting information for this article is available on the WWW under http://dx.doi.org/10.1002/anie.201507620.

clature **A**-**B** was adopted, where **A** represents the number of carbon atoms of phenyl aliphatic groups $R^1$ and **B** is the number of carbon atoms of the ketone aliphatic group $R^2$.

Compound **1-3** with methoxy phenyl and propyl ketone substituents displays gradual transition centered at 230 K, supported also by Mössbauer spectroscopic studies (Supporting Information, Figure S1, S2). The magnetic behavior of **4-1** with butyl phenyl substituents and methyl group of ketone is different and can be described as slightly sensitive to variation of temperature in the whole experimental temperature range (Supporting Information, Figure S1). At low temperature, the susceptibility is close to zero and upon heating increases up to 0.91 $cm^3 K mol^{-1}$ at 400 K. Lengthening aliphatic chains up to $C_8H_{17}$- to produce **8-1** does not change this magnetic behavior (Supporting Information, Figure S1); the magnetic susceptibility of the compound only slightly increases on approaching 400 K.

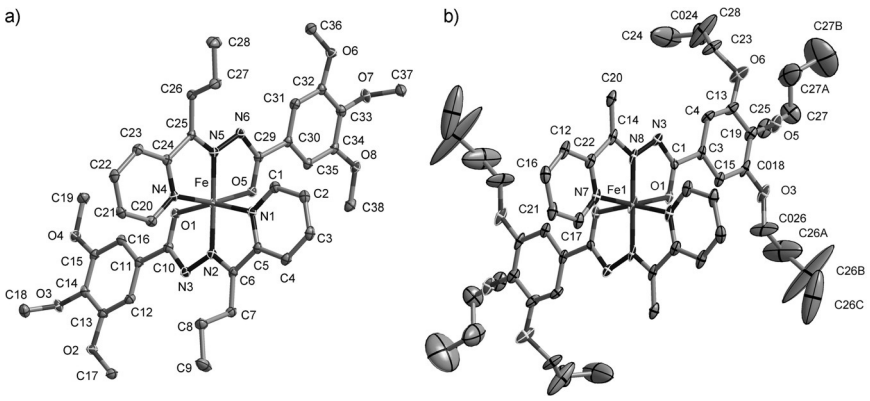


***Figure 1.*** Molecular structure of **1-3** (a) and **4-1** (b) both at 120 K at 50% and 30% probability ellipsoids, respectively. The hydrogen atoms are omitted for clarity.

Single crystal studies of **1-3** reveal that the $Fe^{II}$-center is located in a distorted octahedral $N_4O_2$ coordination environment of the two ligand molecules (Figure 1a; Supporting Information, Table S1). At 120 K, the average bond lengths, Fe–N = 1.912(2) Å and Fe–O = 2.0146(14) Å, are within the region reported for LS $Fe^{II}$ complexes of the similar type, while at 300 K the corresponding values, 2.134(4) Å and 2.080(3) Å, are characteristic for the HS state (Supporting Information, Figure S3).[16] Only one relevant intermolecular contact below the corresponding sum of van der Waals radii[17] is observed between the carbon atoms of the pyridine and phenyl rings: C4···$C13^{i}$ (*i*: $1-x$, $-y$, $-z$) and C23···$C32^{ii}$ (*ii*: $1-x$, -y, $1-z$) equal to 3.307(3) and 3.346(3) Å, respectively (Figure 2a). The corresponding centroid–centroid distance equals to 4.698(3) Å and is far beyond viable interactions. Apparently, the absence of strong intermolecular contacts is responsible for observed gradual transition.

Although a detailed discussion of the structure of **4-1** is not possible owing to poor quality of the crystals resulting from strong disorder of butyl groups, the structural analysis discloses peculiarities of the crystal packing owing to longer phenyl aliphatic chains, and explains the different magnetic behavior in comparison with **1-3** (Supporting Information, Table S1). As well as for its congener at 120 K, the two substituted tridentate ligand molecules form a complex molecule with the average Fe–N and Fe–O bond lengths of **4-1** equal to 1.898(8) Å and 1.972(5) Å, respectively, attributable to the LS state. Because of the asymmetric substitution of the ligand, the phenyl aliphatic chains of the complex molecule are protruding in one direction, while the coordination part remains undecorated (Figure 1b). This enables effective displaced π-π stacking between coplanar pyridine rings of neighbor molecules organized in one-dimensional supramolecular chains (Figure 2b) with centroid–centroid distance of 3.989(10) Å. The separation between neighbor complexes equals to $c/2 = 7.676(6)$ Å, and the interchain distance coincides with cell parameter $a = 8.7624(3)$ Å. Complex molecules **1-3** and **4-1** are essentially similar; therefore, the different packing is responsible for distinct magnetic behavior. This is reminiscent of the phenomenon of polymorphism generating strikingly different spin transitions for different polymorphs.[18]

Further lengthening of aliphatic chains led to the discovery of a very particular effect described below. The magnetic data expressed in the form of $\chi_M T$ vs $T$ ($\chi_M T$ is the molar magnetic susceptibility and $T$ is the temperature) collected at the rate of 1 K $min^{-1}$ for the compounds **14-1**, **14-2**, **14-4**, and **14-5** are shown in Figure 3a. At low temperature, the susceptibility of the four compounds is near to zero, as expected for $Fe^{II}$ ions in the LS state, determined from the Mössbauer data of **14-1** at 80 K (see inset in Figure 3a; it consists of one LS

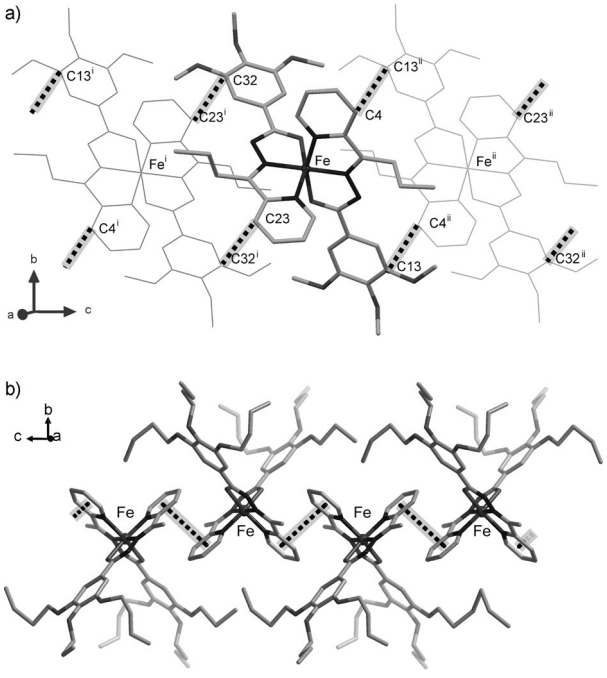


***Figure 2.*** Crystal packing of **1-3** (a) and **4-1** (b).

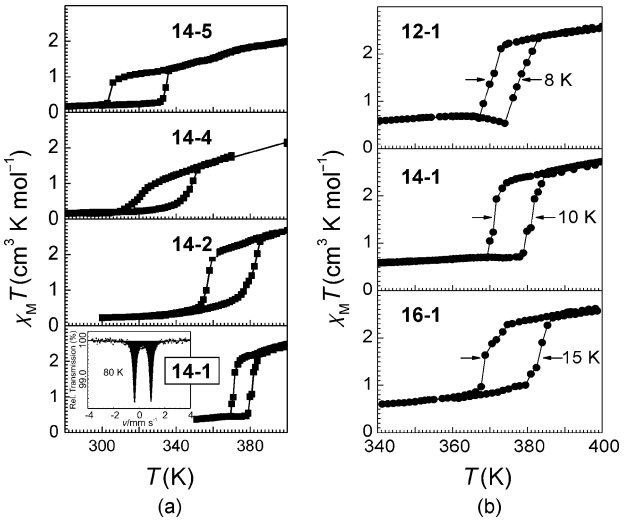


***Figure 3.*** (a) Temperature dependence of $\chi_M T$ for indicated complexes; (b) Variation of hysteresis width for indicated complexes. The inset corresponds to the Mössbauer spectrum of **14-1**.

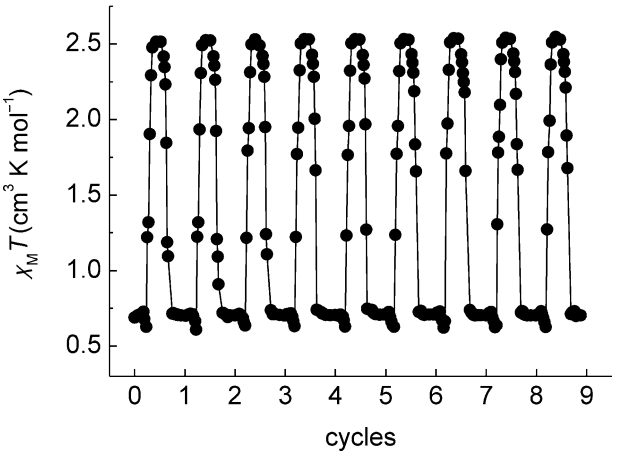


***Figure 4.*** Cycling of the $\chi_M T$ value for **14-1** in temperature range 360–390 K showing robustness of the spin transition.

doublet with parameters $\delta = 0.28(1)$ mm s$^{-1}$, $\Delta E_Q = 1.28(1)$ mm s$^{-1}$)). Upon heating up to 381 K, the susceptibility of this compound jumps to 2.1 cm$^3$ K mol$^{-1}$, and continues gradually to increase up to 400 K. The cooling curve does not coincide with the heating curve since the abrupt decrease of the susceptibility takes place at 371 K. The center of the shaped hysteresis is located at 376 K. Decreasing the scan rate to 0.2 K min$^{-1}$ does not change substantially the hysteresis shape, but increasing the rate to 4 K min$^{-1}$ does, at which point the hysteresis width increases as well as the hysteresis becomes distorted (Supporting Information Figure S4).

The complexes **14-2**, **14-4**, and **14-5** behave similarly, with the center of the hysteresis at 369, 333, and 319 K, serially. The hysteresis width increases in the series and is 10, 24, 25, and 30 K, serially, that is, is the smallest for **14-1** and the largest for **14-5**. On the other hand, the percentage of $Fe^{II}$ ions changing spin state is the largest for **14-1** (ca. 60 %) and is the smallest for **14-5** (ca. 30 %), while intermediate values are observed for **14-2** and **14-4**. Interestingly, upon changing the aliphatic chains -$C_{14}H_{29}$ in **14-1** to -$C_{12}H_{25}$ (compound **12-1**) or -$C_{16}H_{33}$ (compound **16-1**), the center of hysteresis remains at about 376 K, but the hysteresis width can be fine-tuned between 8 K and 15 K (Figure 3b). Also worth stressing, the spin transition is perfectly reproducible over nine cycles of heating–cooling in the 350–390 K temperature range, exhibiting robustness and absence of fatigue (Figure 4).

In relation to these observations, differential scanning calorimetry (DSC) experiments reveals the presence of the exothermic/endothermic processes on the cooling/warming paths, respectively, peaked at similar temperatures to those obtained from the magnetic data of the compounds (Supporting Information, Table S2, Figure S5). The evaluated variation of enthalpy ($\Delta H$) and entropy ($\Delta S$) far exceed the corresponding typical values for strong cooperative SCO transitions (that is, $\Delta H = 20$ kJ mol$^{-1}$ and $\Delta S = 93$ J K$^{-1}$ mol$^{-1}$).[19] The thermodynamic values observed for the title compounds point out further high-energetic processes synchronized with the spin transition. Supposedly, the observed decreasing of $\Delta H$ and $\Delta S$, and averaged transition temperature $<T^{\uparrow\downarrow}>$ from **14-2** to **14-4** and **14-5**, is in accordance with the decreasing interchain interactions owing to increasing size of lateral ketone substituent $R^2$, which, however, does not influence the observed synchronicity between the spin and phase transitions.

The XRD characterization of fresh long chain complexes manifests highly crystalline lamellar structure at 300 K, since the profiles render well separated angle peaks starting from the peak with Miller index (20) and weaker ones up to the 12th order (Supporting Information, Figure S6). The number of carbon atoms plotted against the interlayer distance calculated for **12-1**, **14-1**, **16-1**, and for **4-1** (from the single-crystal structure) gives points lying on one line (Supporting Information, Figure S7), a fact that confirms their similar structural arrangement. The diffractograms of all substances manifest a cluster of peaks at $2\theta \approx 21°$, typical for compounds with the paraffinic sublattice.[20] To understand the structural change taking place at the temperatures of the spin transition, a series of XRD profiles of **14-1** was measured sequentially (Figure 5). A fresh sample retains crystallinity up to 380 K,

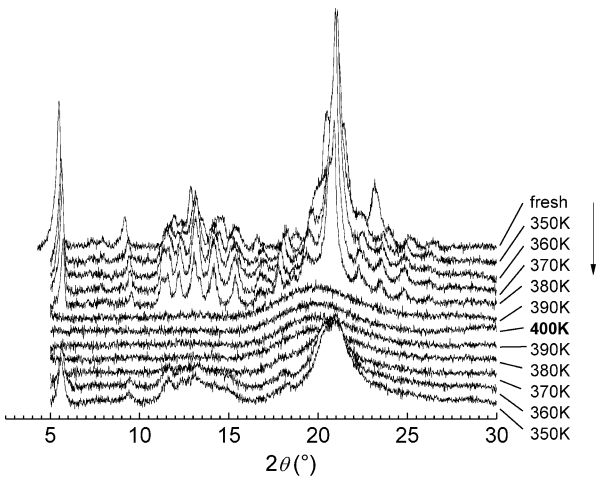


***Figure 5.*** A series of XRD profiles of **14-1** on heating and subsequent cooling.

where the profile loses all reflections except the broad alkyl halo at $2\theta = 20°$. This type of profile is attributed to the isotropic liquid state of the compound after passing the melting point.[13] Upon subsequent cooling, the crystal-like character of the XRD profile is recovered owing to crystallization of the compound. The above data clearly demonstrate that the spin transition of **14-1**, as well as all of the other long-chain compounds under discussion, is triggered by the crystal-to-liquid phase transition (Supporting Information, Figure S8).

Polarized optical microscopy above the melting point confirms the liquid nature of **14-1**, which forms an optically inactive phase and flows, but at lower temperatures in crystalline state resists shearing. Figure 6 collects microphotograph of crystallization process in a thin film of **14-1**, resulting in formation of dark colored solid LS phase (see the Supporting Information). The thermochromism and solubility of the compounds in chloroform encouraged us to check their processability for making a thermochromic device. A filter paper was soaked in a chloroform solution of **14-1**, dried and deposed over heating elements forming letters UV (Figure 6; Supporting Information). When the current is on, the produced heat switches the color of the absorbed compound to green-yellow owing to melting and the resulting spin transition LS-to-HS, while switching off the current and resulting cooling to ambient temperature solidifies the compound and reverses the color back to green resulting from spin transition HS-to-LS.

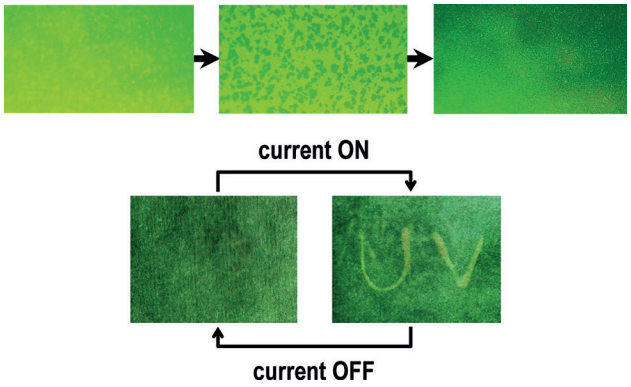


***Figure 6.*** (Top) Microphotographs of crystallization process in a film of molten **1**–**14** showing nucleation and grow of dark colored LS crystals (8× magnification); (Bottom) Thermal switching of **14-1** soaked to filter paper.

In summary, the reported $Fe^{II}$ compounds exhibit abrupt and perfectly reversible spin transitions upon melting to liquid phase. The structural characterization discloses formation of supramolecular structure supposedly generated by π-π stacking interactions between molecules, which stabilizes the LS state of complex molecules in the solid state. The melting to liquid results in the disappearance of ordered supramolecular structure (that is, break of intermolecular contacts), followed by an abrupt change in behavior of $Fe^{II}$ ions at the melting point. Remarkably, the temperature of melting–solidification point is defined by the length of the side ketone substituent $R^2$, while the hysteresis width of the phase transition is a function of the length of aliphatic phenyl substituents $R^1$, of the ligand. We expect that these results can be extended to other ST compounds, which will lead to a useful strategy for synthesizing and processing new spin transition materials in the future.

## Acknowledgements

This work was supported by the Spanish Ministerio de Economia y Competitividad (MINECO) and FEDER funds (CTQ2013-46275-P), the Generalitat Valenciana through PROMETEO/2012/049. T.R.M. thanks the MINECO for a predoctoral (FPI) grant. M.S. thanks the EU for a Marie Curie Fellowship (IIF-253254). We gratefully acknowledge Dr. G. Molnár for Mössbauer measurements, and Prof. Dr. Y. Galyametdinov for preliminary microscopic studies.

**Keywords:** magnetism · phase transitions · soft matter · spin transitions · thermochromism

**How to cite:** *Angew. Chem. Int. Ed.* **2015**, *54*, 14777–14781
*Angew. Chem.* **2015**, *127*, 14990–14994

[1] a) C. Chong, H. Mishra, K. Boukheddaden, S. Denise, G. Bouchez, E. Collet, J. C. Ameline, A. D. Naik, Y. Garcia, F. Varret, *J. Phys. Chem. B* **2010**, *114*, 1975; b) F. Varret, C. Chong, A. Slimani, D. Garrot, Y. Garcia, A. D. Naik, *Spin-Crossover Materials*, Wiley, Hoboken, **2013**, pp. 425.

[2] a) A. Bousseksou, G. Molnar, P. Demont, J. Menegotto, *J. Mater. Chem.* **2003**, *13*, 2069; b) T. Guillon, S. Bonhommeau, J. S. Costa, A. Zwick, J. F. Létard, P. Demont, G. Molnar, A. Bousseksou, *Phys. Status Solidi A* **2006**, *203*, 2974.

[3] a) F. Prins, M. Monrabal-Capilla, E. A. Osorio, E. Coronado, H. S. J. van der Zant, *Adv. Mater.* **2011**, *23*, 1545; b) A. Rotaru, I. y. A. Gural'skiy, G. Molnár, L. Salmon, P. Demont, A. Bousseksou, *Chem. Commun.* **2012**, *48*, 4163; c) Y.-C. Chen, Y. Meng, Z.-P. Ni, M.-L. Tong, *J. Mater. Chem. C* **2015**, *3*, 945.

[4] a) P. Gütlich, A. Hauser, H. Spiering, *Angew. Chem. Int. Ed. Engl.* **1994**, *33*, 2024; *Angew. Chem.* **1994**, *106*, 2109; b) M. A. Halcrow, *Spin-Crossover Materials*, Wiley, Hoboken, **2013**, pp. 147.

[5] a) K. S. Murray, C. J. Kepert, *Top. Curr. Chem.* **2004**, *233*, 195; b) H. Banerjee, M. Kumar, T. Saha-Dasgupta, *Phys. Rev. B* **2014**, *90*, 174433.

[6] a) H. Spiering, T. Kohlhaas, N. Romstedt, A. Hauser, C. Bruns Yilmaz, J. Kusz, P. Gütlich, *Coord. Chem. Rev.* **1999**, *190–192*, 629; b) M. Sorai, *Bull. Chem. Soc. Jpn.* **2001**, *74*, 2223; c) M. Sorai, M. Nakano, Y. Miyazaki, *Chem. Rev.* **2006**, *106*, 976; d) O. Sato, J. Tao, Y. Z. Zhang, *Angew. Chem. Int. Ed.* **2007**, *46*, 2152; *Angew. Chem.* **2007**, *119*, 2200.

[7] O. Kahn, J. Martinez, *Science* **1998**, *279*, 44.

[8] R. Ohtani, K. Yoneda, S. Furukawa, N. Horike, S. Kitagawa, A. B. Gaspar, M. C. Muñoz, J. A. Real, M. Ohba, *J. Am. Chem. Soc.* **2011**, *133*, 8600.

[9] a) H. Constant-Machado, J. Linares, F. Varret, J. G. Haasnoot, J. P. Martin, J. Zarembowitch, A. Dworkin, A. Bousseksou, *J. Phys. I* **1996**, *6*, 1203; b) T. Tayagaki, A. Galet, G. Molnar, M. C. Muñoz, A. Zwick, K. Tanaka, J. A. Real, A. Bousseksou, *J. Phys. Chem. B* **2005**, *109*, 14859; c) R. Tanasa, C. Enachescu, A. Stancu, J. Linares, E. Codjovi, F. Varret, J. Haasnoot, *Phys. Rev. B* **2005**, *71*, 014431.

  

[10] a) V. Ksenofontov, A. B. Gaspar, P. Gütlich, *Top. Curr. Chem.* **2004**, *235*, 23; b) P. Guionneau, E. Collet, in *Spin-Crossover Materials*, Wiley, Hoboken, **2013**, pp. 507; c) A. B. Gaspar, G. Levchenko, S. Terekhov, G. Bukin, J. Valverde-Muñoz, F. J. Muñoz-Lara, M. Seredyuk, J. A. Real, *Eur. J. Inorg. Chem.* **2014**, 429.

[11] a) I. Boldog, A. B. Gaspar, V. Martínez, P. Pardo-Ibáñez, V. Ksenofontov, A. Bhattacharjee, P. Gütlich, J. A. Real, *Angew. Chem. Int. Ed.* **2008**, *47*, 6433; *Angew. Chem.* **2008**, *120*, 6533; b) F. Volatron, L. Catala, E. Rivière, A. Gloter, O. Stephan, T. Mallah, *Inorg. Chem.* **2008**, *47*, 6584; c) V. Martínez, I. Boldog, A. B. Gaspar, V. Ksenofontov, A. Bhattacharjee, P. Gütlich, J. A. Real, *Chem. Mater.* **2010**, *22*, 4271; d) H. Peng, S. Tricard, G. Félix, G. Molnár, W. Nicolazzi, L. Salmon, A. Bousseksou, *Angew. Chem. Int. Ed.* **2014**, *53*, 10894; *Angew. Chem.* **2014**, *126*, 11074; e) M. Giménez-Marqués, M. L. García-Sanz de Larrea, E. Coronado, *J. Mater. Chem. C* **2015**, *3*, 7946.

[12] a) M. Seredyuk, A. B. Gaspar, V. Ksenofontov, Y. Galyametdinov, J. Kusz, P. Gütlich, *Adv. Funct. Mater.* **2008**, *18*, 2089; b) M. Seredyuk, A. B. Gaspar, V. Ksenofontov, Y. Galyametdinov, J. Kusz, P. Gütlich, *J. Am. Chem. Soc.* **2008**, *130*, 1431; c) M. Seredyuk, M. C. Muñoz, V. Ksenofontov, P. Gütlich, Y. Galyametdinov, J. A. Real, *Inorg. Chem.* **2014**, *53*, 8442.

[13] Y. H. Lee, A. Ohta, Y. Yamamoto, Y. Komatsu, K. Kato, T. Shimizu, H. Shinoda, S. Hayami, *Polyhedron* **2011**, *30*, 3001.

[14] A. B. Gaspar, M. Seredyuk, *Coord. Chem. Rev.* **2014**, *268*, 41.

[15] L. Zhang, G. C. Xu, H. B. Xu, V. Mereacre, Z. M. Wang, A. K. Powell, S. Gao, *Dalton Trans.* **2010**, *39*, 4856.

[16] L. Zhang, G.-C. Xu, Z.-M. Wang, S. Gao, *Eur. J. Inorg. Chem.* **2013**, 1043.

[17] A. Bondi, *J. Phys. Chem.* **1964**, *68*, 441.

[18] J. Tao, R.-J. Wei, R.-B. Huang, L.-S. Zheng, *Chem. Soc. Rev.* **2012**, *41*, 703.

[19] M. C. Muñoz, J. A. Real, *Coord. Chem. Rev.* **2011**, *255*, 2068.

[20] D. L. Dorset, *Crystallography of the polymethylene chain: an inquiry into the structure of waxes* (Ed.: D. L. Dorset), Oxford University Press, Oxford, New York, **2005**.

Received: August 14, 2015
Published online: October 16, 2015

  